A LIQUID SCINTILLATOR CALORIMETER FOR THE FORWARD REGION OF AN LHC EXPERIMENT

A. Artamonov, V. Epstein, P. Gorbunov, V. Jemanov, V. Khovansky, S. Kruchinin, A. Maslennikov, M. Rjabinin, V. Zaitsev, S. Zeldovich, I. Zuckerman
ITEP, Moscow, Russia.

V. Barassi, S. Buontempo, A. Ereditato, G. Fiorillo, F. Garufi
Universita' "Federico II" and Sezione INFN, Naples, Italy.

Abstract

We report on the design and on beam test results of a liquid scintillator/lead prototype calorimeter. The detector was proposed as one of the options for the forward region of an experiment at the future Large Hadron Collider (LHC) at CERN. The measurements were performed with electron and pion beams of the CERN SPS in the energy range from 20 to 150 GeV. The response as a function of the beam impact point and of the incidence angle is studied with and without passive preradiator in front of the calorimeter modules.

1. INTRODUCTION

The main challenge for a forward calorimeter in an LHC experiment is the high radiation dose it must withstand, up to 1 MGy/year at $|\eta| = 5$, for an integrated luminosity of 10^5 pb^{-1} [1]. This requires the use of radiation-hard materials, efficient protection of the read–out electronics, and the protection (or replaceability) of those parts of the calorimeter which cannot be made radiation hard. Monte Carlo simulations show that the hadronic energy resolution and the lateral granularity are not critical parameters for forward calorimetry; a hadronic energy resolution of about $100\%/\sqrt{E(GeV)} \oplus 10\%$ is adequate to accomplish the task [1, 2]. On the other hand, due to the high interaction rate, the detector speed is an important issue.

The above constraints restrict the choice of suitable calorimetric techniques. In this paper, we discuss about a calorimeter whose active medium is liquid scintillator circulating in quartz tubes embedded in a lead matrix which acts as passive material [3]. In this case, the replacement of the active medium is therefore possible.

2. CALORIMETER DESIGN AND CONSTRUCTION

The description of the LHC full scale design of the calorimeter can be found elsewhere [1]. It has modular structure; in the following, we describe the design, the construction and the tests performed on individual modules and on a prototype assembly composed of four modules. The module has parallelepiped shape with

66×66 mm^2 cross–section and 2380 mm length, including a 380 mm long photodetector housing (Fig.1). The housing is lightproof and contains a photomultiplier (PM) with a light mixer in front of it. The mixer (150 mm long) is used to distribute the light over the 2" PM photocathode surface. The module itself consists of a lead matrix confining 81 quartz tubes; their inner diameter is 2.8 mm and the wall thickness 300 μm. All tubes run parallel to one another along the module axis; they are arranged in a square transverse pattern with a 7.3 mm center-to-center spacing providing about 6:1 lead–to–liquid volume ratio. The choice of such a volume ratio should result in e/h close to unity [4].

The modules were constructed from grooved lead plates produced by casting. Stainless steel tubes 2010 mm long with inner diameter of 3.8 mm and wall thickness of 200 μm were placed in the grooves, and the lead plates were glued together using special 100 μm thick tape which was put under and above the tubes. The assembly underwent some compression and high temperature, the compression being released after the glue hardening. The tubes, coming out at both ends of the module, were inserted into holes drilled in stainless steel manifolds and then tin soldered; the front manifold has inlet and outlet pipes separated by a membrane, while the back one is provided with a frame with a glass window to transmit the scintillation light to the light detectors.

Modules were washed with purified alcohol flow circulated by a pump within a few hours and dried with air; then, 2100 mm long quartz tubes were inserted in the tubes from the back module end. The last 10 cm of the tube back ends were bent to form a bundle with a 42×42 mm^2 cross–section.

Prior to filling with the liquid scintillator, the modules were blown with inert gas. After filling, the liquid was circulated by a pump to remove the bubbles. Then, the outlet pipe was connected to a buffer volume by 1/3 filled with the scintillator and by 2/3 with the gas.

3. THE LIQUID SCINTILLATOR

In order to study issues related to the module filling and the liquid circulation through the tubes, we built a test device consisting of 1.5 m long transparent glass tubes assembled in the same way as the module tubes. The liquid flow in individual tubes was watched by adding a dye to the transparent fluid pumped through the device. Tests showed that laminar flow without stagnation can be obtained if a membrane is placed in the middle of the front manifold. The membrane separates the module in two halves in which the liquid flows in opposite directions. It is worth mentioning that the high irradiation dose expected at the LHC is absorbed in a few percent of the entire volume of the forward calorimeter. Calculations show that, at a flow speed of 20 $cm/hour$, the liquid scintillator in the "hottest" modules ($D_{peak}^{year} = 1$ MGy) will be exposed to 1 kGy before being stirred up in the recycling system.

We measured light yield and light transmission in single tubes filled with two commercial liquid scintillators, MN+R45 [5] (methylnaphtalene based) and BC599-13G [6] (IBP based). Both liquids are hydrocarbons with high refraction index, emitting in green.

The finite light attenuation length contributes to the constant term in the hadronic energy resolution because of fluctuations in the longitudinal shower development. The intrinsic attenuation length of $200 - 250\ cm$ of these two scintillators is insufficient to achieve a constant term lower than 10%. However, the attenuation length can be increased up to $5\ m$ by using yellow-orange filters in front of the PM (see Fig.2) at the price of a reduction of the light yield. We will come back in detail to this question later.

The measurements were performed adopting two different methods. In the first approach we used a ^{106}Ru radioactive source of moderate intensity. The collimated electrons crossed the tube and were absorbed in a thick trigger counter. The light from the tube was detected by a PM. The signal was amplified and digitized by an ADC. The obtained charge distributions were used to calculate the corresponding number of photoelectrons for different distances of the source from the PM. In the second method, the tube was irradiated by an intense ^{90}Sr beta source. The PM average current was measured for different positions of the source along the tube. The last method is more effective in case of very few photoelectrons per minimum ionizing particle (m.i.p.), particularly when filters are used. Both methods give comparable results, summarized in Fig.2.

4. EXPERIMENTAL SET-UP AND DATA

The beam test results described below come from two different sets of measurements performed in 1993 and 1994. In 1993, two modules filled with MN+R45 were first tested with cosmic rays and then placed in the H2 beam of the SPS at CERN. They were installed side by side on a movable support with the tubes parallel to the beam direction. Particles were sent onto the detectors at various angles in the horizontal and vertical planes, θ_x and θ_y. Five scintillation trigger counters and two Delay Wire Chambers (DWC) were installed upstream. The trigger signal was built from the coincidence of either all five or only three counters. The resulting beam spots were, respectively, square of $5 \times 5\ mm^2$ or round with $20\ mm$ diameter. The DWCs provided the measurement of the impact point position on the module front faces with an accuracy better than $0.5\ mm$. The modules were exposed to electron beams with energies of 20, 40, 80 and $150\ GeV$ hitting the center of one of them at different angles. A lateral scan across the boundary between the modules was also performed. We shall refer to this set-up as "$1 + 1$".

In 1994, a test set-up, which we shall refer to as "2×2" assembly, was composed of three newly built modules and one of those used in the 1993 tests. The new modules were filled with BC599-13G. The total assembly cross-section was

$132 \times 132\ mm^2$. To achieve the desired hadronic energy resolution, all the modules were equipped with filters, chosen to provide an attenuation length of about $4\ m$. The modules were tested with cosmics, and the beam tests were performed in the H6 SPS beam with 20, 40, 80, 120 GeV electrons and pions.

The assembly was placed on a movable table allowing displacements in the vertical or horizontal direction, and tilts in the horizontal plane. A sketch of the experimental set-up is shown in Fig. 3. A veto counter and two 'finger' scintillation counters $S2$ and $S3$ were placed two meters upstream. The overlap of the last two counters defined the beam spot size of $7 \times 7\ mm^2$. The trigger signal was given by their coincidence. The counters $S2$ and $S3$ were followed by a passive preradiator of a few X_o, used to improve the lateral uniformity of the response to electrons. A $60 \times 50\ mm^2$ counter $S4$ was installed just in front of the assembly. With preradiator in place, the pulse height of this counter was used to discriminate between pions and electrons. In the electron (pion) runs the resulting pion (electron) contamination was found to be 0.4 (0.8)%. The modules were followed by two scintillation counters to detect passing through muons. All beam counters were read-out for the subsequent off-line event selection. Data were taken with an ADC gate of $200\ ns$.

The response of individual modules was equalized by hitting electrons and pions into the center of each module. The peak values of the resulting signal distributions were taken as equalization constants. Thus, two different sets of constants were obtained, one from electrons and one from pions. The further analysis showed that the results are almost insensitive to the choice of the set of constants.

5. RESULTS

5.1 MEASUREMENTS WITH COSMIC RAYS

The light produced by a m.i.p. and the attenuation length were measured by means of cosmic muons crossing the modules. Results for the "$1+1$" set-up are given in Figs.4 and 5. The observed light yield at $100\ cm$ distance from the PM is equivalent to about 20 photoelectrons. The effective light attenuation length is about $200\ cm$, in agreement with single tube measurements.

For the "2×2" set-up the attenuation length is in the range $320 \div 440\ cm$, varying from module to module. The measurement uncertainty of $\pm\ 50\ cm$ is essentially due to the low light yield, especially at the module far end. The presence of filters decreases by approximately a factor of 4 the light yield at $100\ cm$ from the PM and, in the case of the BC599-13G liquid (with filter), it corresponds to 2.5 photoelectrons per m.i.p. This is equivalent to about 25 photoelectrons per GeV of shower energy, largely sufficient to achieve the aimed stochastic term.

5.2 RESPONSE TO ELECTRONS

Because of the high energy, the resolution of a forward calorimeter at the

LHC is dominated by the constant term. A 10% constant term for single hadrons seems to be adequate to meet the physics goals [1]. Since neutral pions carry, on average, one third of the jet energy, an electromagnetic constant term as large as 15% is sufficient.

Examples of the response to 80 GeV electrons hitting the centre of the module at different angles θ with the module axis are given in Fig.6 for the "$1+1$" set-up. The non-gaussian shape of the distributions is due to the coarse sampling frequency of the module. Using the position information provided by the beam chambers one finds that, for particles hitting a tube, the response is higher compared to the one of particles hitting the absorber. The less is the incidence angle and the higher the energy, the more distinct becomes the two-peak structure in the response distribution. The peaks can be disentangled by selecting particles according to the distance of their impact point from the center of the tube. This is illustrated in Fig.7 for $\theta = 1^o$ and 80 GeV energy.

We performed a scan, in steps of 5 mm, across the boundary of the two adjacent modules at an incidence angle of 2.9^o in the vertical plane. Fig.8 shows the response to 80 GeV electrons as a function of the X impact point. Alternating minima and maxima correspond to the 7.3 mm center-to-center distance between the tubes. The 10% drop, in the proximity of the boundary, can be attributed to the 1 mm crack between the modules along the first 50 cm, caused by the imperfect shape of one of the modules.

The energy resolution discussed in this section is defined as r.m.s./mean of the corresponding distributions. Fig.9 presents the resolution as a function of the particle incidence angle θ at 20 and 80 GeV. The points with close values of θ were obtained at different θ_x and θ_y. The resolution is almost flat above $\theta = 5^o$ but it deteriorates significantly towards zero. Fig.10 shows the energy dependence of the resolution at 2^o and 4.9^o, relevant angles for a forward calorimeter at the LHC. The quadratic fit exhibits a slightly better agreement with the data than the linear one. From the figure one can conclude that, with this set-up, the constant term for electrons is within the $10 - 20$ % range.

The energy dependence of the response to electrons was studied for different incidence angles. The results are given in Fig.11. The signals at fixed angle are found to be linear over the energy range $20 - 150$ GeV. It turns out that the signal per GeV at $\theta = 2^o$ is 5% higher that the one at 4.9^o.

With the "2×2" set-up, the response to electrons was studied for two incidence angles. The beam was sent at the center of the assembly. The calorimeter response is defined in this case as the sum of the four module signals. The effect of the preradiator is illustrated in Fig.12 (a) showing the signal distributions for 120 GeV electrons at 1^o, with and without $3X_o$ preradiator. The preradiator eliminates the high signal tail and reduces the distribution spread by 50%. Fig.12 (b) shows distributions with preradiator at 1^o and 3^o incidence angles. As expected, the increase of the angle results in a higher energy resolution.

The effect of different preradiator thickness has also been studied. Fig.13 shows that the resolution improves with the increasing thickness, while the response is almost constant in the explored range.

Fig.14 shows the calorimeter response as a function of the beam energy for two incidence angles, with a $3X_o$ preradiator. The non-linearity is likely to be due to lateral leakage caused by the preradiator itself. The point at $80\ GeV$ was excluded because of beam line setting problems experienced during the data taking.

The energy resolution as a function of the energy is shown in Fig.15. A linear fit to these points gives

$$\sigma(E)/E = (74 \pm 4)\%/\sqrt{E(GeV)} + (12 \pm 0.4)\%$$

at 1^o and

$$\sigma(E)/E = (50 \pm 2)\%/\sqrt{E(GeV)} + (11 \pm 0.4)\%$$

at 3^o.

5.3 RESPONSE TO PIONS

The "2×2" set-up was exposed to pion beams at two different incidence angles, 0^o and 1^o. The prototype cross-section was not sufficiently large to ensure full lateral containment of hadronic showers. Two different Monte Carlo codes, FLUKA and GHEISHA (both in the framework of GEANT 3.15 [9]), predict similar values for the energy leakage with this set-up: 49% and 42% respectively for tilt angle of 1^o and beam energy of $120\ GeV$. However, the two programs disagree in the predictions of the e/π ratio: FLUKA predicts a significant overcompensation with $e/\pi \sim 1/1.7$, while, according to GHEISHA, this type of calorimeter should be nearly compensating. In our design, the $6:1$ lead-to-scintillator volume ratio was chosen to provide a slight ($\sim 10\%$) overcompensation.

We assessed the e/π ratio of the fully containing calorimeter by correcting the measured value 1.34 ± 0.05 for the different light attenuation for electron and pion induced showers (a factor 1.14 for $\lambda = 4\ m$) and for the energy leakage (a factor 0.58, assuming the GHEISHA prediction). GHEISHA also predicts $(e/\pi)_\infty = 0.89 \pm 0.06$ at 1^o tilt angle and $120\ GeV$ beam energy, in agreement with the design value and in contrast to FLUKA. For these reasons, we used GHEISHA for further analysis.

Fig.16 shows the response distribution to $120\ GeV$ pions. The low energy tail is due to lateral leakage and is well described by the Monte Carlo simulation.

The response and resolution energy dependence are shown in Fig.17. Unlike for the electrons, the resolution for pions is obtained from a gaussian fit to the distributions in a $\pm 2\sigma$ region around the peak. By a linear fit to the experimental points, one obtains the following energy dependence of the resolution

$$\sigma(E)/E = (86 \pm 11)\%/\sqrt{E(GeV)} + (7.3 \pm 1.2)\%\ ,$$

which is in fair agreement with the predictions of GHEISHA:

$$\sigma(E)/E = (83 \pm 12)\%/\sqrt{E(GeV)} + (4.5 \pm 1.5)\%$$

The simulation of a fully containing calorimeter gives

$$\sigma(E)/E = (56 \pm 10)\%/\sqrt{E(GeV)} + (8.7 \pm 1.4)\% \ ,$$

which well matches the design goal for a forward calorimeter at the LHC (see e.g. [1]).

6. CONCLUSIONS

We have tested the performance of a liquid scintillator prototype calorimeter designed for the forward region of an LHC experiment. The calorimeter has a modular structure. Each module consists of quartz tubes, filled with liquid scintillator, embedded into a lead matrix which acts as passive material.

Tests demonstrated that laminar liquid flow without stagnation can be obtained, thus solving the problem of the calorimeter operation in high radiation environments ($\sim$ 1 MGy/year).

The design goal is to achieve a hadronic energy resolution of about $100\%/\sqrt{E(GeV)} \oplus 10\%$. Coarse sampling frequency, resulting from the relatively large tube diameter required to provide laminar flow, makes difficult to obtain the same (low) constant term for electromagnetic showers.

The beam tests with electrons showed that the module response exhibits a transverse non-uniformity of about $\pm 15\%$. The resolution is significantly improved when a passive preradiator of a few X_o is placed $2\ m$ upstream. With the preradiator an electron energy resolution

$$\sigma(E)/E = (50 \pm 2)\%/\sqrt{E(GeV)} + (11 \pm 0.4)\%$$

was obtained, at 3^o incidence angle.

The assembly of 2×2 modules used in the beam tests was not sufficiently large to contain hadronic showers. Therefore, the hadronic energy resolution could not be studied in detail. The measured resolution for pions was found to be

$$\sigma(E)/E = (86 \pm 11)\%/\sqrt{E(GeV)} + (7.3 \pm 1.2)\%$$

in agreement with the GHEISHA expectations. This makes us confident in the Monte Carlo prediction of

$$\sigma(E)/E = (56 \pm 10)\%/\sqrt{E(GeV)} + (8.7 \pm 1.4)\%$$

for a fully containing calorimeter.

Acknowledgements

We wish to thank L. Poggioli for his invaluable help in the preparation of the 1993 beam test. We also thank our technicians A. Utenkov and A. Zokhov for their efforts in preparing the modules, following the very tight time schedule. Funding of INFN is also acknowledged.

REFERENCES

1. ATLAS. Letter of Intent for a General-Purpose pp Experiment at the LHC at CERN, CERN/LHCC/92-4, LHCC/I 2
2. SDC collaboration, Technical Design Report, SDC-92-201.
3. A. Artamonov et al., in Proc. II Int. Conf. on Calorimetry in High Energy Physics, 1991, Capri, Ed. A. Ereditato, World Scientific, Singapore, 1992
4. D. Acosta et al., Nucl. Instr. and Meth. **A308** (1991) 481
5. GEOSPHAERA Research Center inc., Moscow, Russia
6. BICRON Corporation, Newbury, Ohio, USA
7. A.Artamonov et al., in Proc. III int. Conf. on Calorimetry in High Energy Physics, 1992, Corpus Christi, Ed. P. Hale and J. Siegrist, World Scientific, Singapore, 1993
8. A. Artamonov et al., to be published in proc V Int. Conf. on Calorimetry in High Energy Physics, 1994, Brookhaven
9. CERN Program Library Long Writeup Q123.

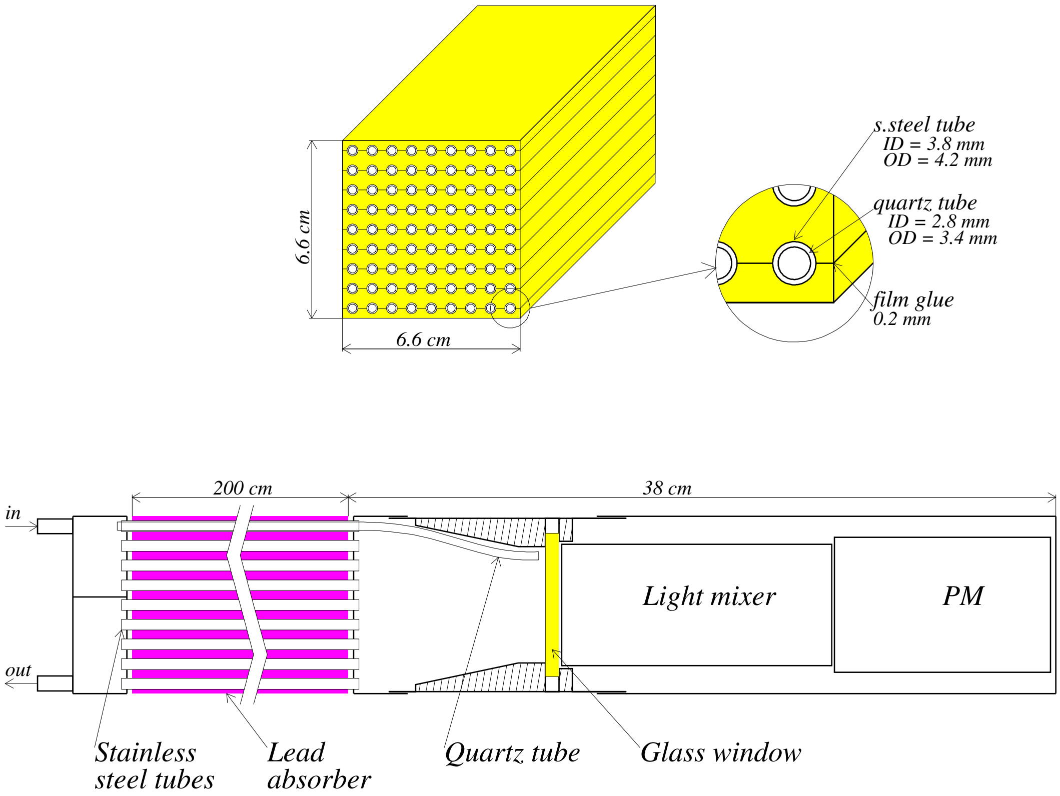

Figure 1: *Calorimeter module design*

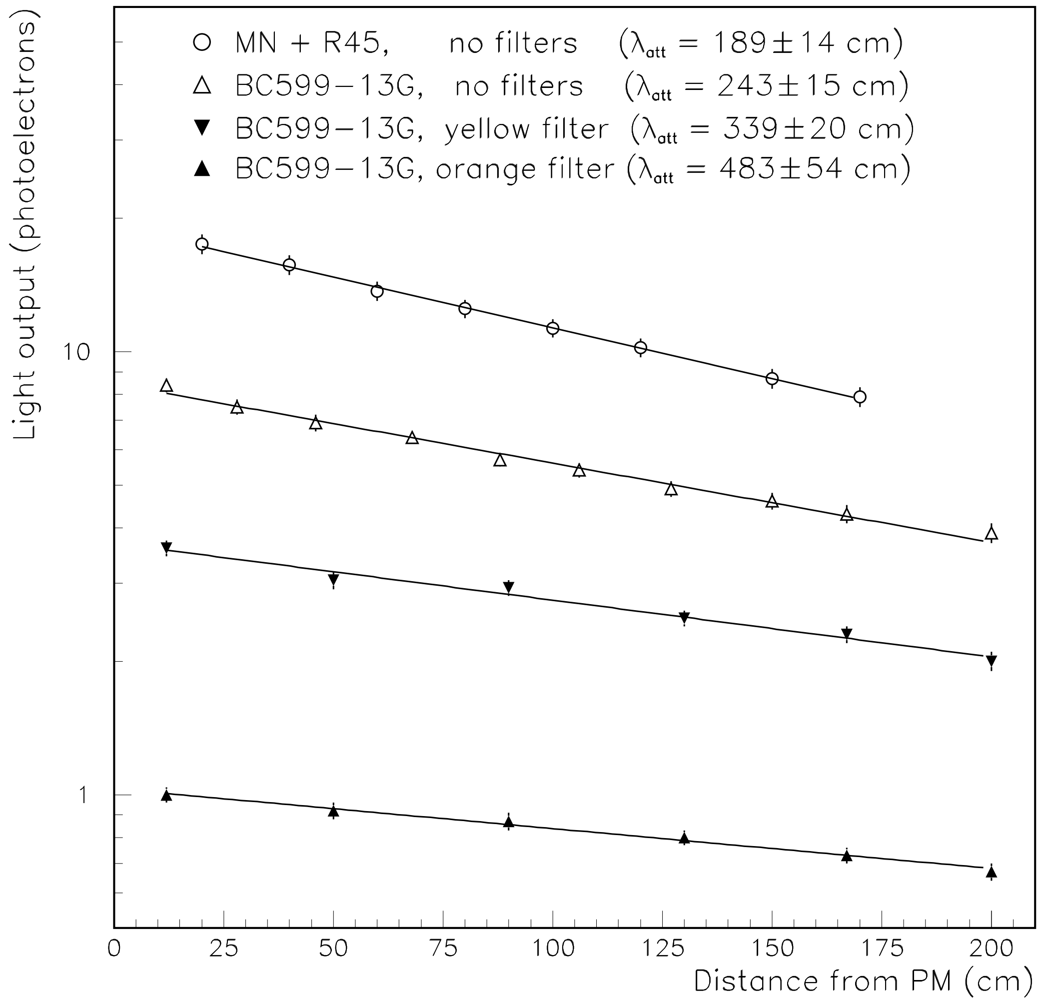

Figure 2: *Light yield as a function of the distance from the PM for MN+R45 and BC599-13G scintillators. For the latter the effect of filters is also shown*

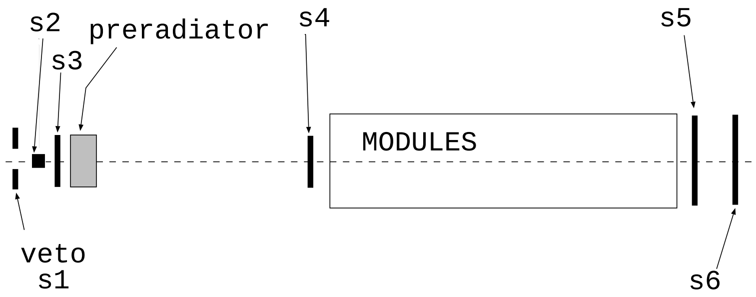

Figure 3: *Position of modules and counters along the beam line for the "2×2" set-up*

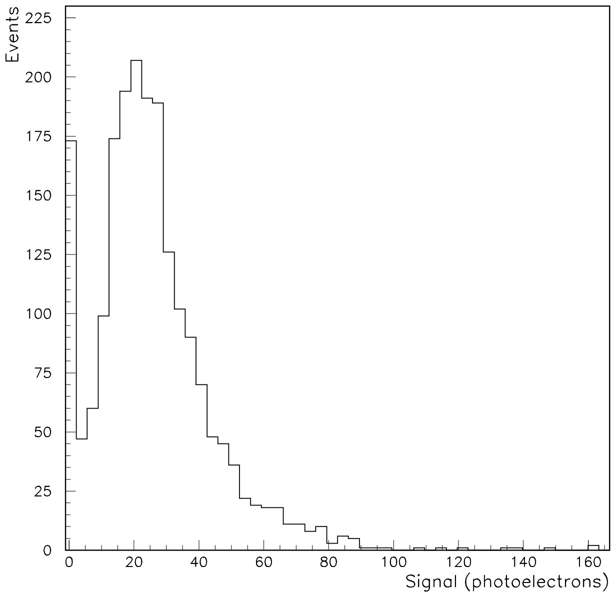

Figure 4: *The results of measurements with cosmic muons: pulse height distribution measured at 15 cm from the PM photocathode*

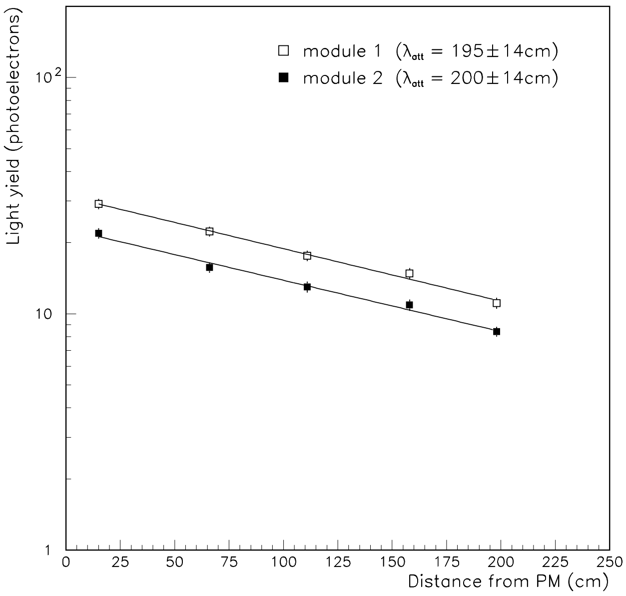

Figure 5: *Light yield in the modules vs the distance from the PM photocathode*

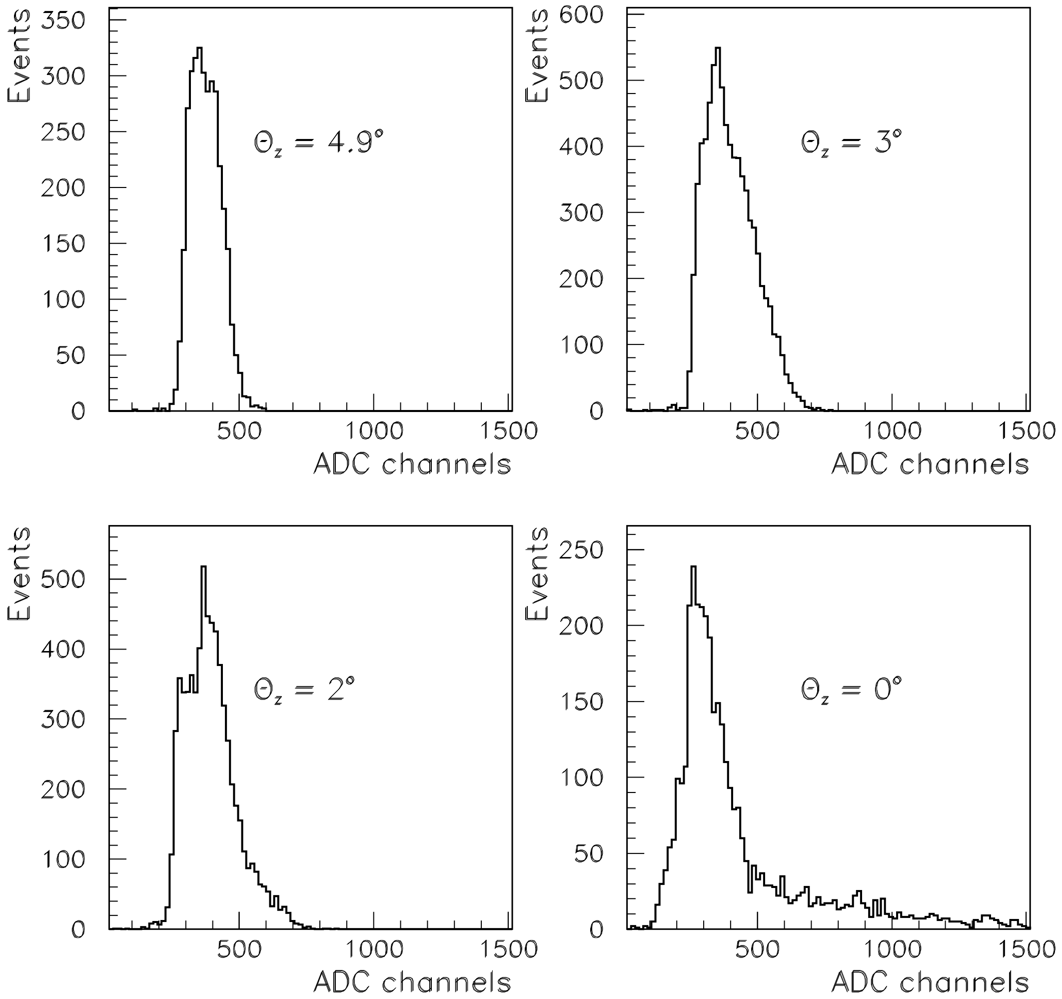

Figure 6: *Signal distribution for 80 GeV electrons at different angles*

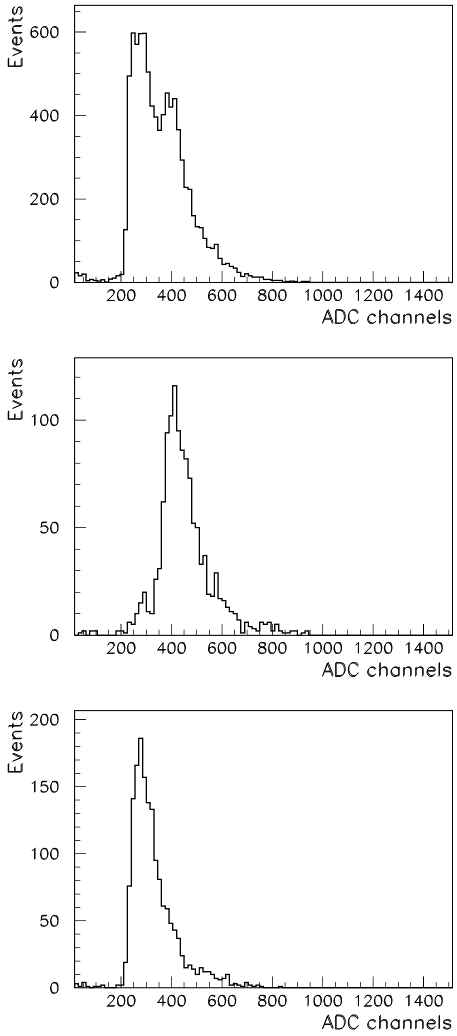

Figure 7: *Signal distributions for 80 GeV electrons entering the module at $\theta_z = 1^o$. Top - all events, middle - events with the impact point within 2.4 mm distance from the center of the tube, bottom - events with the impact point distance between 3.4 and 4.8 mm from the center of the tube*

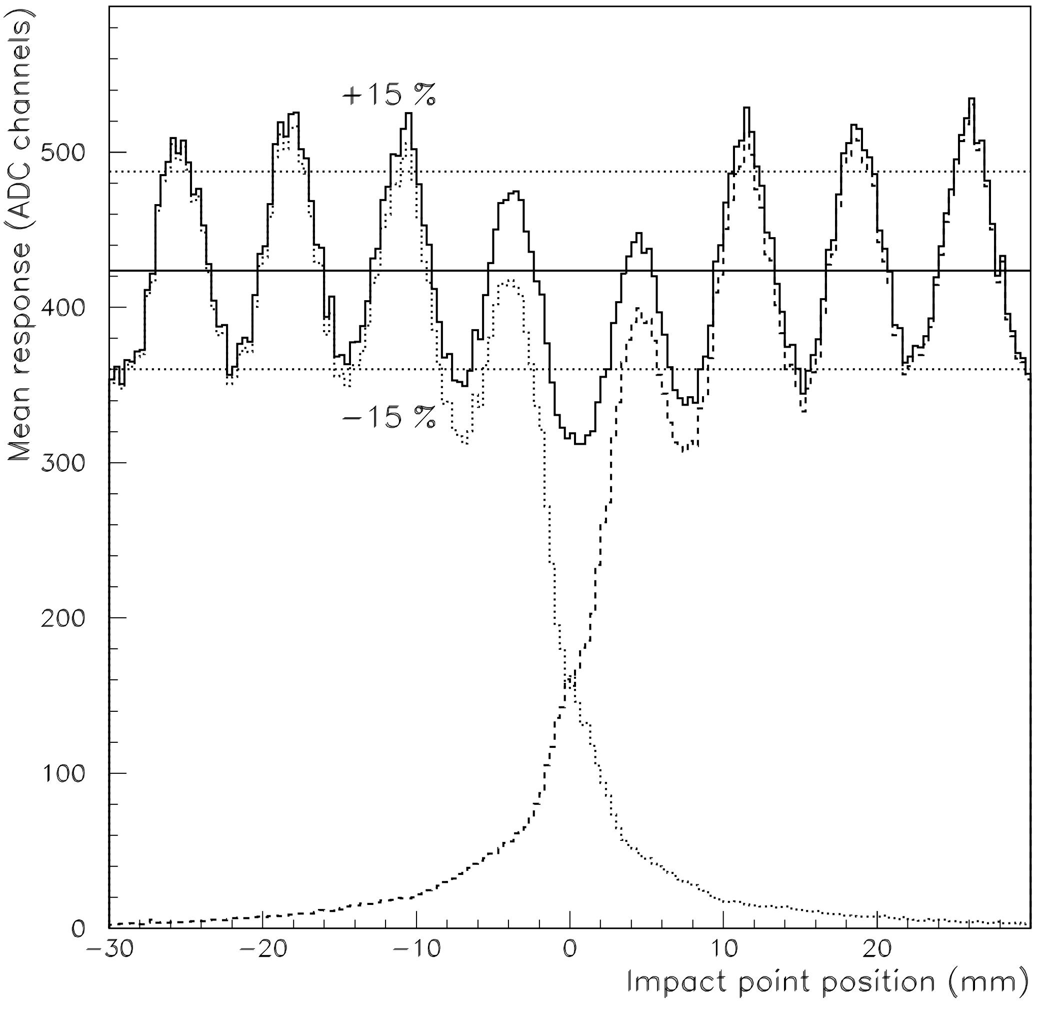

Figure 8: *Response to 80 GeV electrons as a function of the X impact point position.* $\theta_z = \theta_y = 2.9^o$

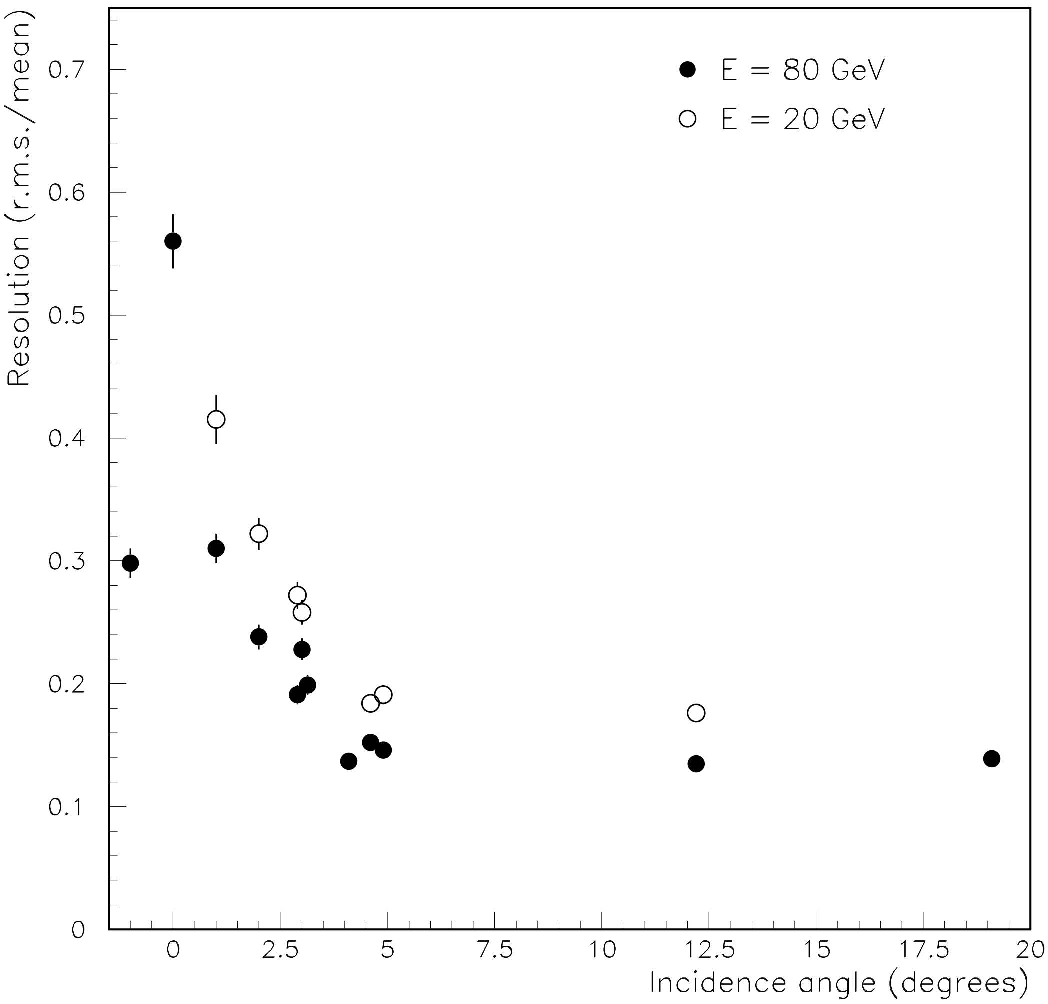

Figure 9: *The resolution for electrons as a function of the incidence angle*

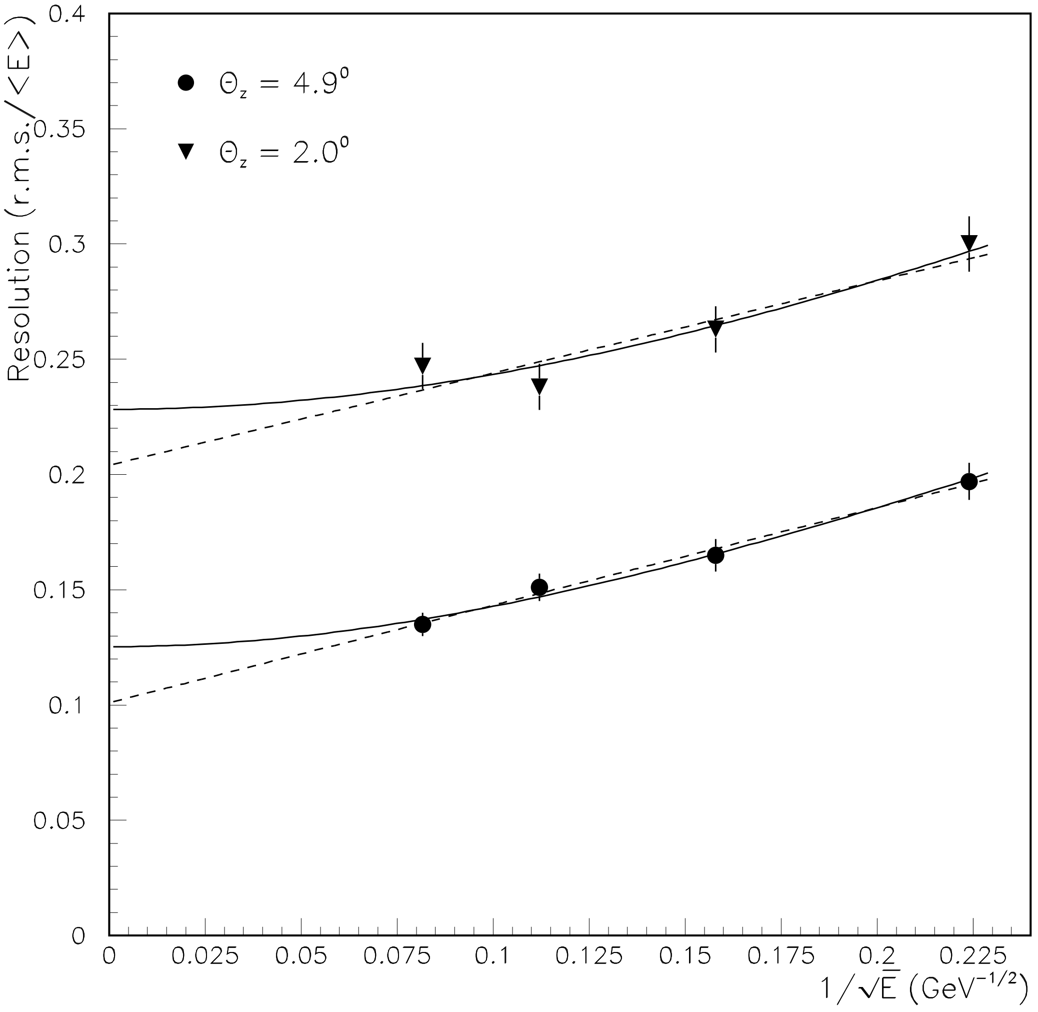

Figure 10: *The resolution for electrons as a function of the beam energy: continuous curve quadratic fit; dashed curve linear fit ("$1+1$" set-up)*

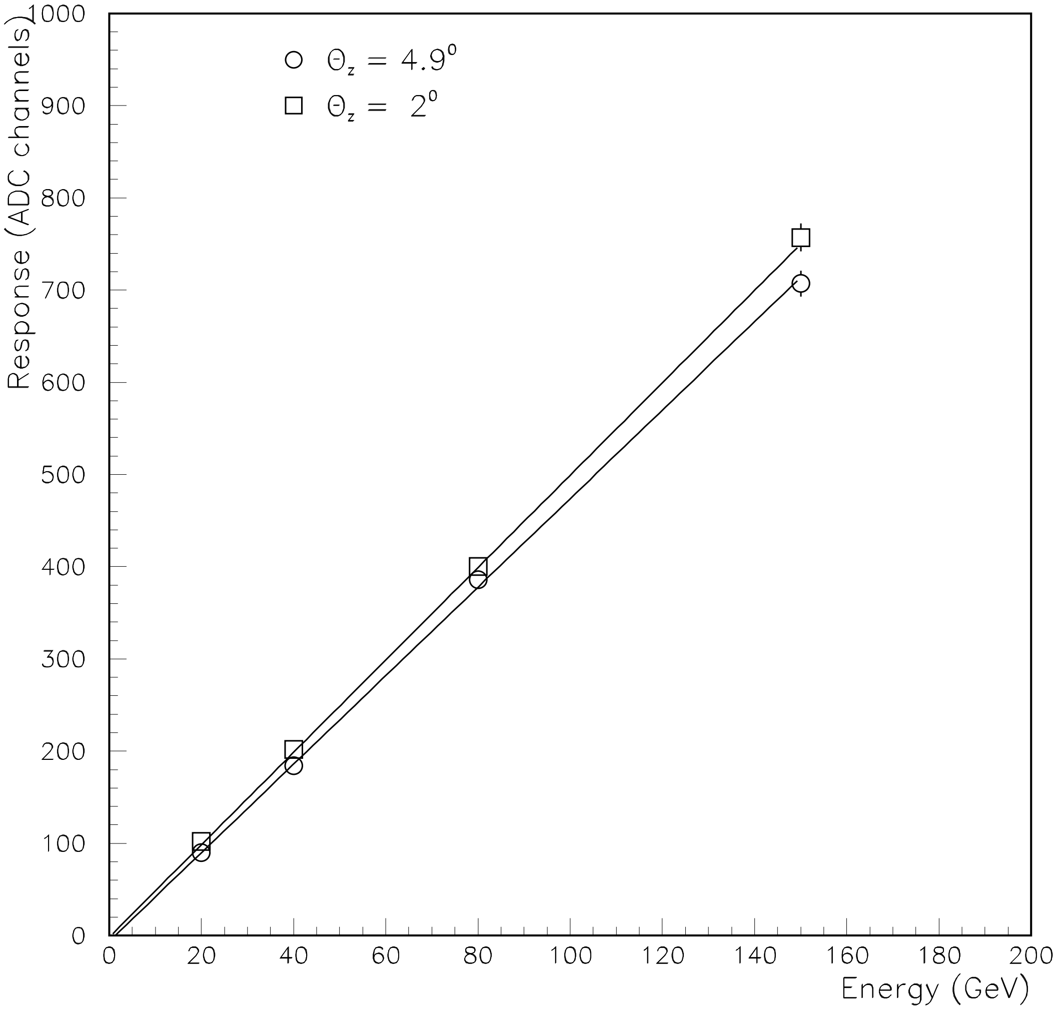

Figure 11: *Signal energy dependence for electrons at different θ_z ("$1+1$" set-up)*

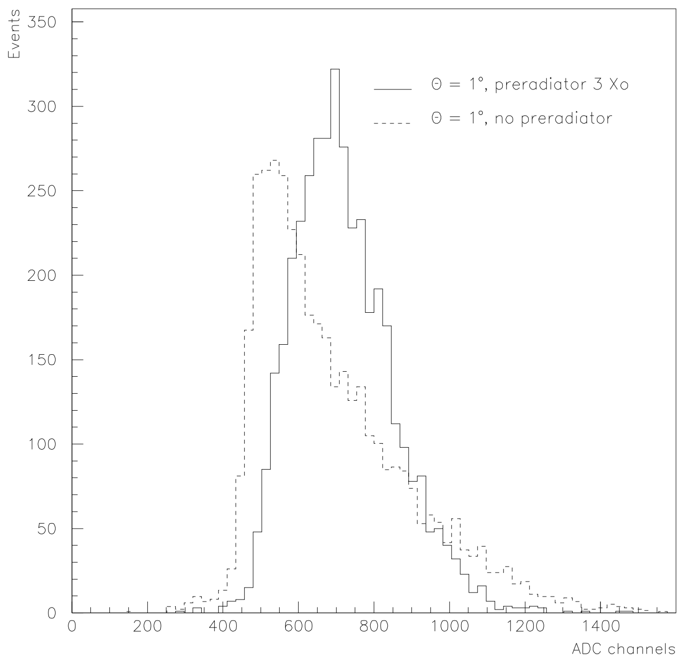

(a)

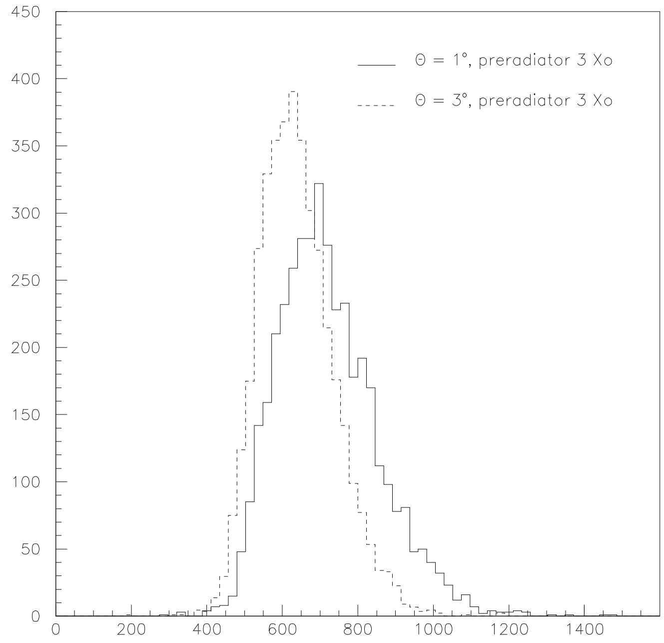

(b)

Figure 12: *(a) Signal distribution for 120 GeV electrons with and without preradiator; (b) distribution with preradiator at two different angles*

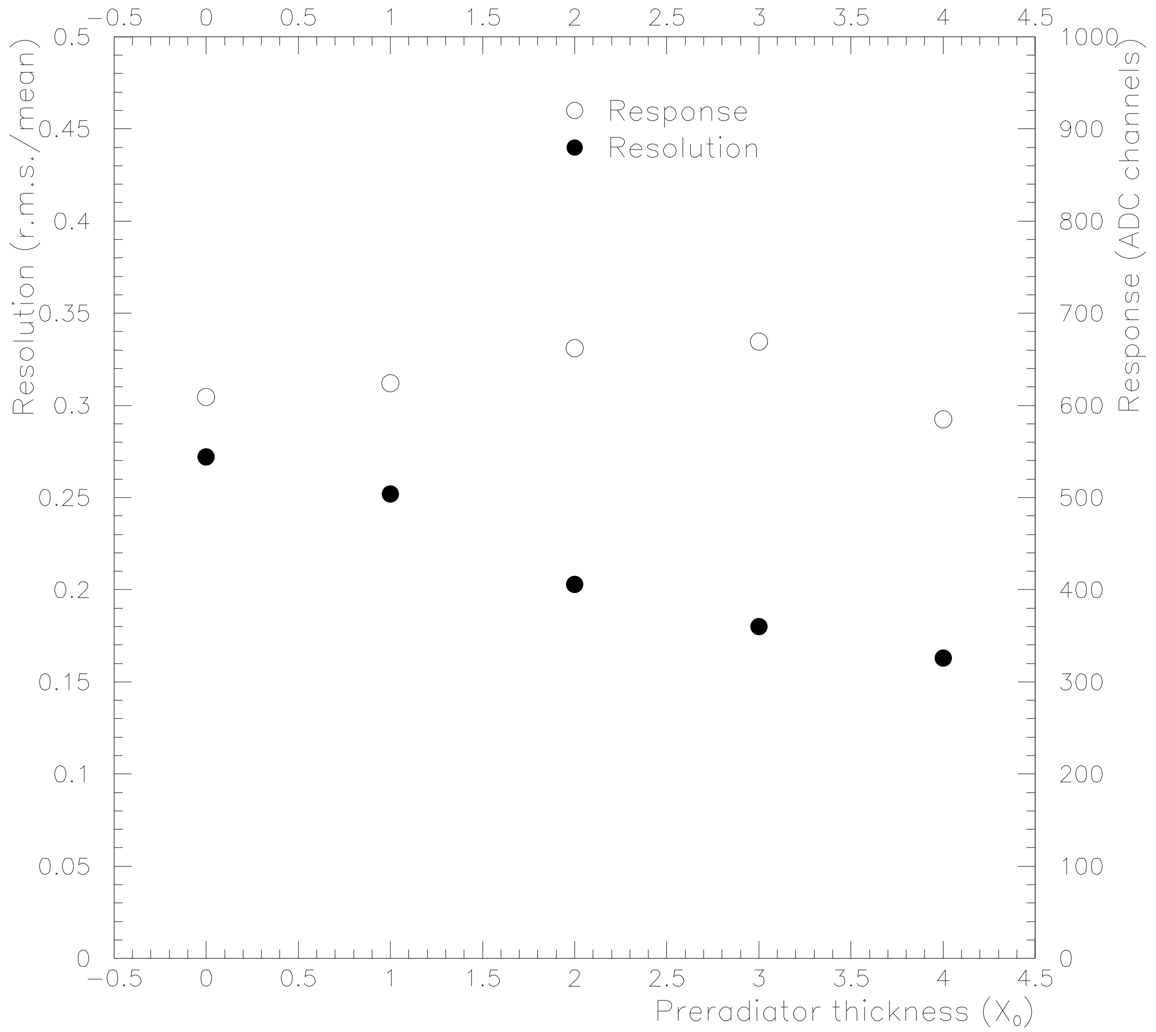

Figure 13: *Energy response and resolution for 120 GeV electrons as a function of the preradiator thickness at $\theta_z = 1^o$*

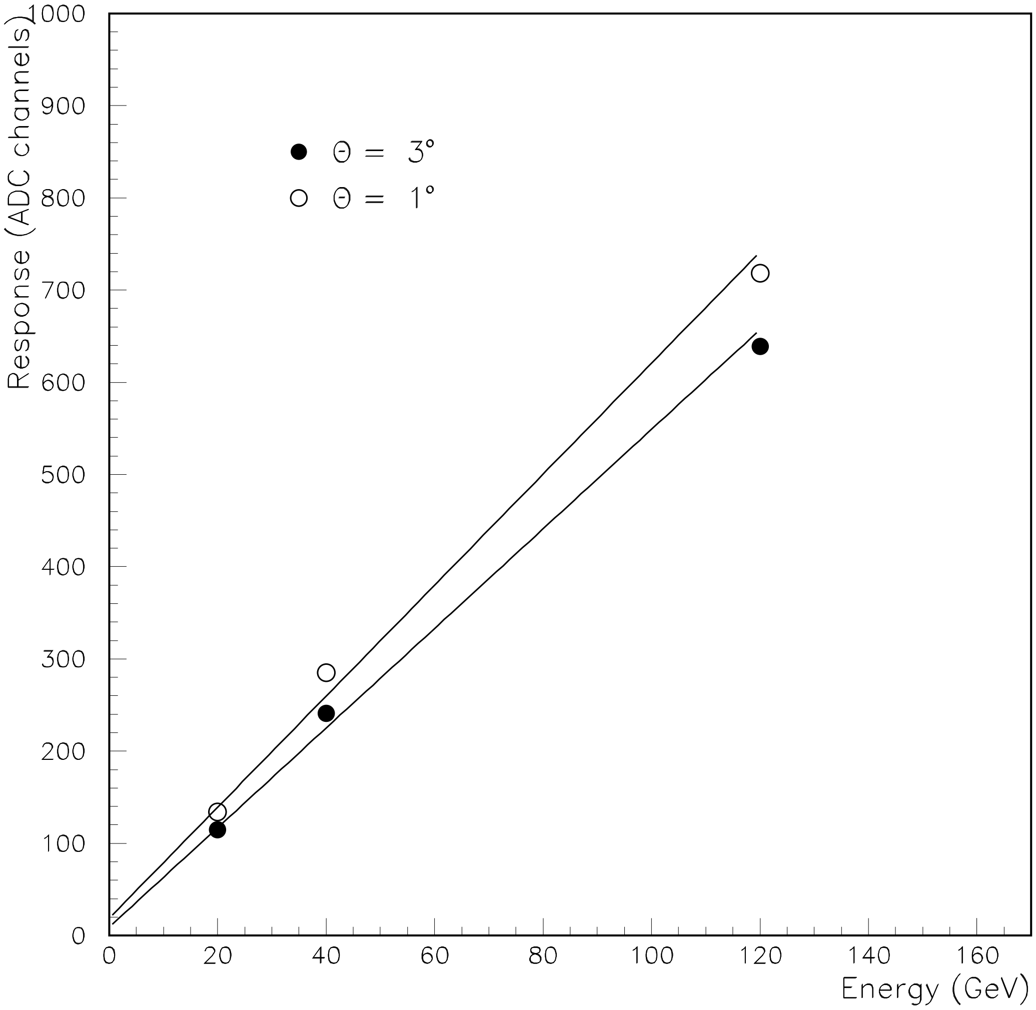

Figure 14: *Signal energy dependence for electrons at different θ_z ("2×2" set-up)*

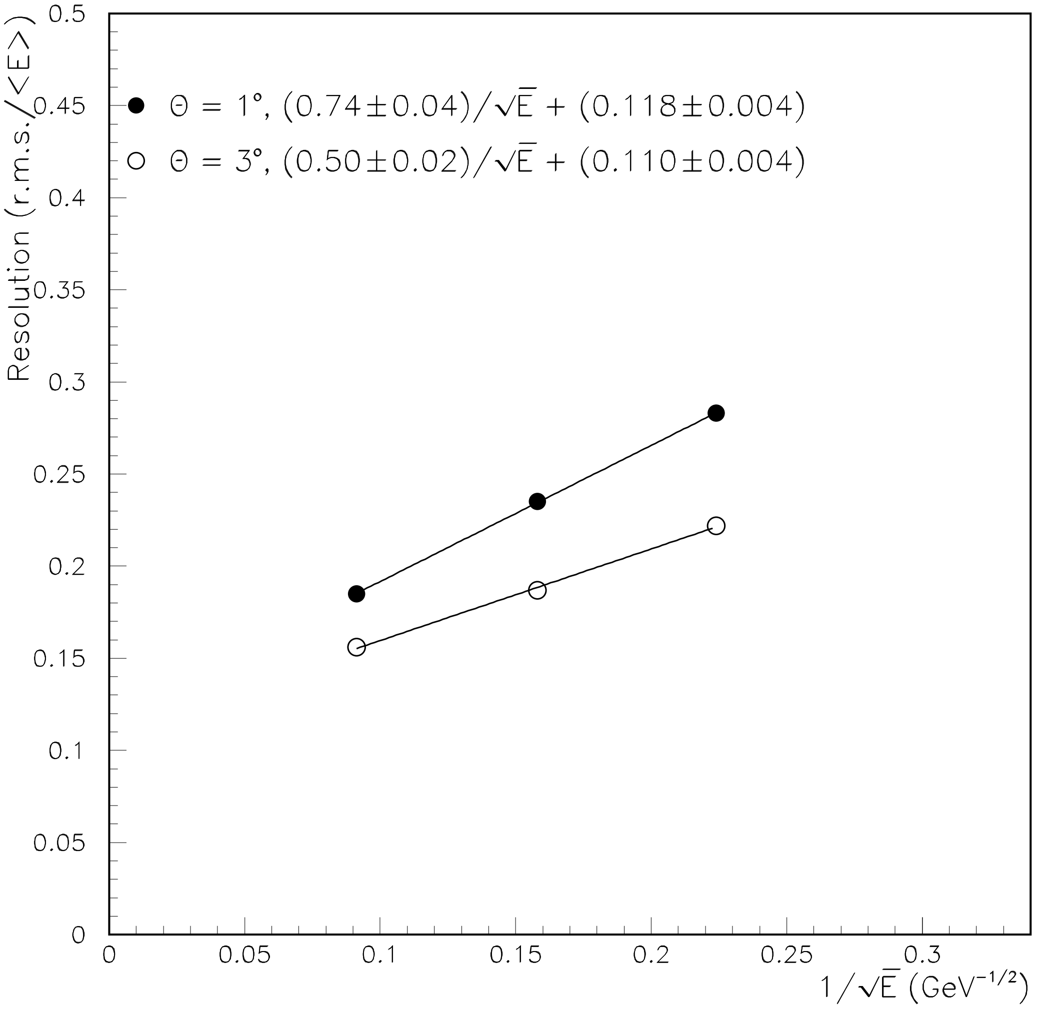

Figure 15: *Electron energy resolution as a function of the energy ("2×2" set-up)*

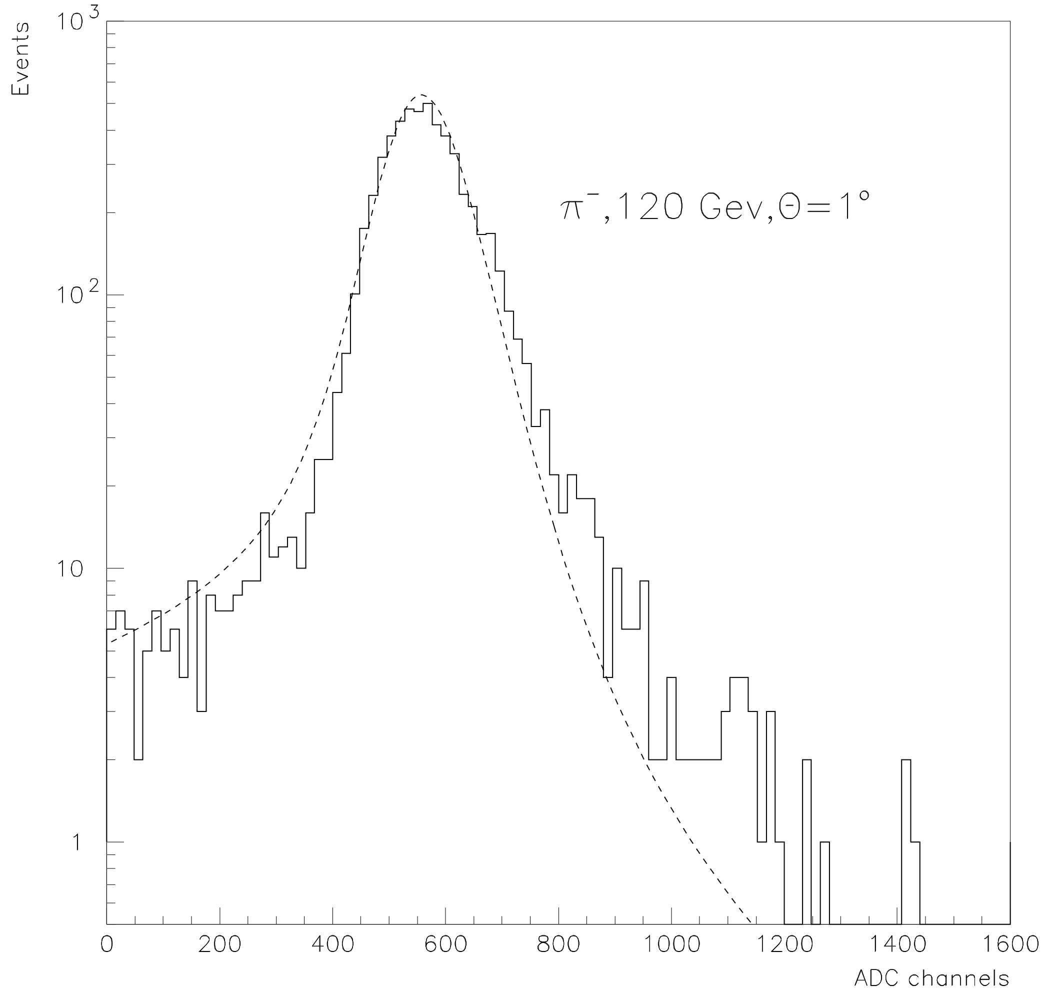

Figure 16: *Energy distribution for 120 GeV pions at θ_z=1°. The dashed line is the prediction of a Monte Carlo simulation*

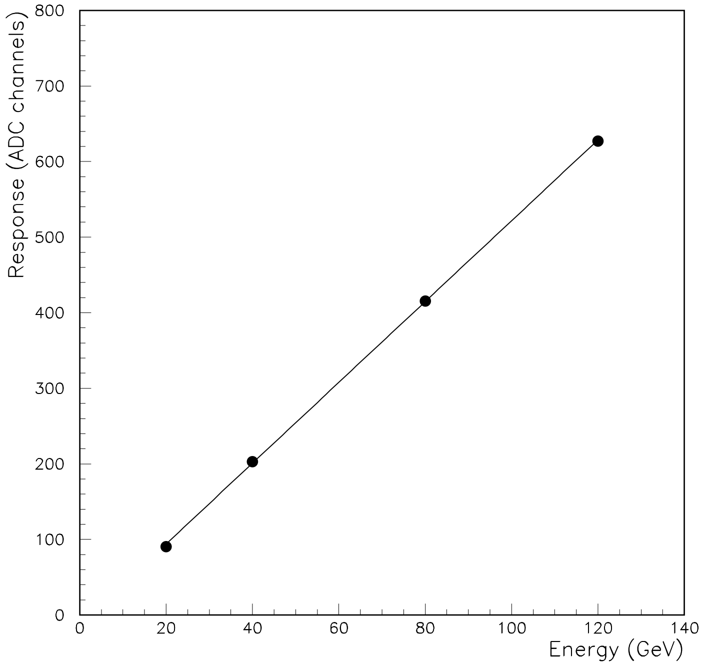

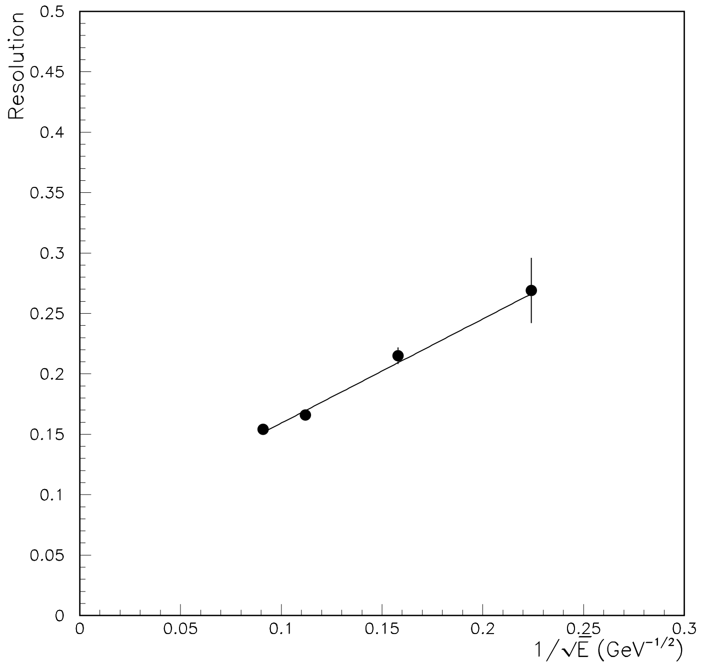

Figure 17: *Pion energy response and resolution as a function of the energy at* $\theta_z = 0^o$